Lead clusters: different potentials, different structures

Jonathan P. K. Doye*

University Chemical Laboratory, Lensfield Road, Cambridge CB2 1EW, United Kingdom

(Dated: February 2, 2008)

The lowest-energy structures of lead clusters interacting via a Gupta potential are obtained for $N \leq 150$. Structures based on Marks decahedra dominate at the larger sizes. These results are very different from those obtained previously using a lead glue potential, and the origins of the differences are related back to differences in the potential.

I. INTRODUCTION

The structure of a metal cluster is one of its most important properties, yet it is a property that can be hard to access for free clusters. Experiments usually lead only to an indirect measurement of the structure, and so results need to be compared to what would be expected for candidate structures. Therefore, there is an important need for reliable predictions from theory. However, this is also something that can be hard to achieve.

For all but quite small clusters, performing a full search for the lowest-energy structure is unfeasible with *ab initio* electronic structure methods. Therefore, one needs to use some kind of potential. However, the energy differences between competing structures can often be relatively small. Furthermore, for a cluster's energy to be accurate, the energetics associated with a wide range of properties potentially need to be well modelled—different external surfaces, twin planes, different crystal structures, and the response to strain. To model the potential temperature dependence of the structure vibrational properties need also to be well described.[1] Therefore, prediction of the correct structure of a cluster represents a tough challenge for a potential. Furthermore, often it is not clear which of the available potentials for a system will work best.

It is my contention that an important aspect of assessing a potential's quality for modelling clusters is to first understand the relationship between the observed structures and the potential. As well as providing fundamental insights into cluster structure, this can help to determine whether the observed structures reflect some robust feature of the potential, or rather whether they stem from some deficiencies in the potential. This is the approach I undertake here. I first find the lowest-energy structures for lead clusters modelled using a Gupta potential, and then compare them to previous results for a lead glue potential.[2] The origins of the differences are explored, highlighting the implications for the relative merits of the two potentials.

II. METHODS

Both potentials that I consider are of the embedded-atom form, where the potential energy is given by

$$
\begin{aligned}
E &= E_{\text{pair}} + E_{\text{embed}} \\
&= \sum_{i<j} \phi(r_{ij}) + \sum_i F(\bar{\rho}_i),
\end{aligned} \tag{1}
$$

where $\phi(r)$ is a short-ranged pair potential, $F(\bar{\rho})$ is a many-body embedding (or glue) function and $\bar{\rho}_i = \sum_j \rho(r_{ij})$, where $\rho(r)$ is an "atomic density" function. One potential is of the Gupta form:[3]

$$
\begin{aligned}
\phi(r) &= 2A e^{-p(r/r_0 - 1)} \\
F(\bar{\rho}) &= -\xi \sqrt{\bar{\rho}} \\
\rho(r) &= e^{-2q(r/r_0 - 1)}.
\end{aligned} \tag{2}
$$

whereas for the glue potential there are no assumed forms for these functions; instead they arise in the fitting process.[4] The parameters of the Gupta potential were fitted on the basis of bulk properties,[3] whereas a much wider variety of configurations, including surface properties, were used to parameterize the glue potential.[4]

However, the functions in Eq. 2 are non-unique. Functions that give rise to exactly the same energy can be constructed by the transformation

$$
\begin{aligned}
\phi'(r) &= \phi(r) + 2g\rho(r) \\
F'(\bar{\rho}) &= F(\bar{\rho}) - g\bar{\rho},
\end{aligned} \tag{3}
$$

This transformation redistributes the total energy between E_{pair} and E_{embed}. When

$$
g = \left. \frac{dF}{d\bar{\rho}} \right|_{\bar{\rho} = \bar{\rho}_{\text{xtal}}}, \tag{4}
$$

$F'(\bar{\rho})$ has a minimum at $\bar{\rho}_{\text{xtal}}$, where $\bar{\rho}_{\text{xtal}}$ is the value of $\bar{\rho}$ in the equilibrium crystal. This choice is called the effective pair format, and has been suggested as the most natural way to partition the energy between the pair and many-body contributions.[5] In this format, when $\bar{\rho} = \bar{\rho}_{\text{xtal}}$ the pair potential controls the energy change for any change of configuration that does not significantly alter $\bar{\rho}$. This form also makes comparisons between different potentials easier.
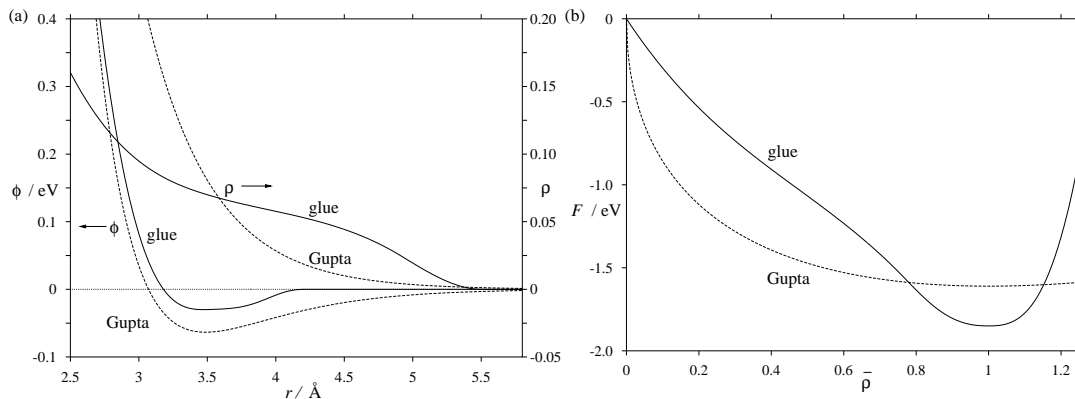
FIG. 1: (a) $\phi(r)$ and $\rho(r)$, and (b) $F(\bar{\rho})$ for lead Gupta and glue potentials in the effective pair format.

Indeed, the components of the two lead potentials are compared in Fig. 1, and are quite different. The pair potential contributes less for the glue potential. At its minimum the energy is only 1.62% of the minimum in the embedding function, compared to 3.94% for the Gupta form. The $\rho(r)$ functions are also very different. For the Gupta potential it decreases rapidly and uniformly because of its exponential form, whereas the glue $\rho(r)$ has a wide plateau around the nearest-neighbour distance.

The optimal clusters will have the best balance between maximizing the pair and embedding energies. As is well-understood,[6] maximization of the pair energy is achieved through a balance between maximizing the number of bonds (i.e. spherical and facets with high coordinate surface atoms, e.g. fcc {111}), and minimizing the strain energy (the energetic penalty for distances that deviate from the minimum of the potential).

The way the embedding energy is maximized and the effects on structure have only begun to be explored more recently.[2,7,8,9,10,11,12] For E_{embed} to be maximal the $\bar{\rho}_i$ for each atom need to be as close to $\bar{\rho}_{\mathrm{xtal}}$ as possible. An important feature is that an atom with a low (high) coordination number can compensate for this by shortening (extending) the bonds. Therefore, the embedding energy will favour a shrinking of the surface, which can in turn compress the interior of the cluster. This can be problematic for structures such as the Mackay icosahedron, where bond distances for surface atoms are longer than interior atoms, and so surface compression can lead to unfavourable energies for the atoms at the core. The magnitude of these effects will depend on the relative depths of the effective pair and embedding functions, as the pair potential will tend to resist any changes in structure that lead to distances deviating from the preferred pair distance. When the embedding energy dominates unusual structures that naturally have bond distances that are shorter on the surface can be favoured.[11,12]

For Gupta potentials the value of p/q provides an approximate indicator of the relative weights of the pair and embedding energies. As p tends to $2q$ the minimum in

the effective pair potential disappears.[12] Therefore, one tends to see a progression from potentials that favour icosahedra to decahedra to close-packed clusters and finally disordered clusters as $p \rightarrow 2q$. This is somewhat simplistic since as one goes further away from $p = 2q$ the other parameters of the potential play an increasing role in the relative depths of the pair and embedding functions.

Global optimization of the lead clusters to locate the lowest-energy structures was achieved using the basin-hopping method,[13] supplemented by reoptimizations of databases of structures found previously for other clusters.[14]

III. RESULTS

Putative global minima up to $N = 150$ were found. For reference, their energies and point groups are given in Table I. The coordinate files for all the global minima can be obtained online at the Cambridge Cluster Database.[14] Results up to N=55 have previously been reported by Lai *et al.*,[15] but the current results improve these at N=43, 50, 51 and 54. The size-dependence of the energies are plotted in Fig. 2, and a selection of clusters are depicted in Fig. 3.

Of the clusters for $N \geq 13$, 70 are decahedral, 29 are close-packed (both perfect face-centred-cubic structures and those involving a twin plane), 6 have a distorted decahedral form recently characterized for zinc and cadmium clusters[12] (e.g. N=16), three are icosahedral and three have polytetrahedral structures. The remaining 27 have no assigned structure, and are somewhat disordered. As is fairly common, these 'disordered' structures appear at the smaller sizes in between the magic numbers at N=13, 38 and 54 that are associated with ordered clusters. Examples at N=23, 30 and 40 are shown in Fig. 3.

Interestingly the uncentred Mackay icosahedron at N=54 is more stable than the usual 55-atom Mackay icosahedron. The strong compressions at the centre of
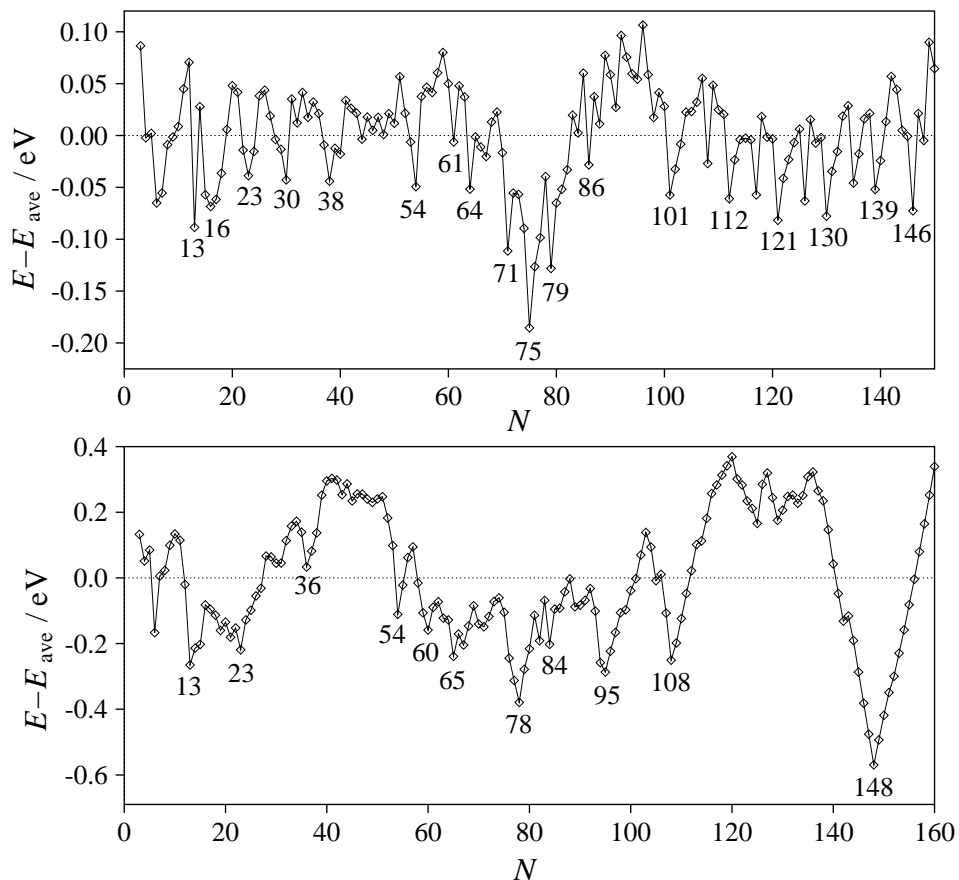
FIG. 2: Energies of the lead clusters modelled by the (a) Gupta and (b) glue potentials relative to E_{ave}, a four-parameter fit to the energies. $E_{\text{ave}}^{\text{Gupta}} = -2.0631N + 0.9778N^{2/3} - 1.0084N^{1/3} + 1.2917$; $E_{\text{ave}}^{\text{glue}} = -2.0251N + 1.6608N^{2/3} + 1.3662N^{1/3} - 0.8634$.

the icosahedron resulting from shrinkage of the surface bonds makes it unfavourable for this site to be occupied. This type of vacancy was first noted by Boyer and Broughton for very large Lennard-Jones Mackay icosahedra,[16] but is not uncommon for much smaller metal clusters because of many-body effects.

For $N \geq 59$ all the clusters are either decahedral or close-packed. A significant proportion of the close-packed clusters are in the region N=85–100, where decahedral clusters with five atoms along the fivefold axis are becoming less stable, yet those with six atoms along this axis are not yet very competitive. It is noticeable that the 75-atom complete Marks decahedron is particularly stable (Fig. 2(a)). However, the other complete Marks decahedra with 101 and 146 atoms are not as prominent in Fig. 2(a) because of their rather prolate and oblate structures, respectively. Indeed, a number of the intermediate asymmetric Marks decahedra have similar stabilities.

The observed structures tally quite well with the value of p/q (2.625). There are fewer disordered and close-packed structures than gold (e.g. $p/q = 2.457$ (Ref. 7)), but less icosahedral and more decahedral structures than for silver (e.g. p/q =3.003 (Ref. 7)).[17] That is, the rela-

tive weights of the embedding and pair terms is such that icosahedra are for the most part not favoured because of unfavourable embedding energies associated with compression of the cluster centre, but decahedra are more prevalent than close-packed clusters because of a more favourable pair energy due to their greater proportion of {111} faces.

When these results are compared to those previously obtained for the glue potential[2] there is virtually no overlap. The pattern of magic numbers is completely different (Fig. 2) and none of the structures are the same for $N \geq 8$. A selection of stable clusters for the glue potential are depicted in Fig. 4 The clusters do not exhibit any of the usual structural forms, and although most are fairly disordered, some strong magic numbers are apparent in Fig. 2(b). The strongest of these is from the highly symmetrical 148-atom hexagonal barrel structure. Also, of interest is the 54-atom cluster as it is related to the uncentred icosahedron favoured for the Gupta potential by a series of twists to the outermost shell around one of the fivefold axes.

The long-range character of $\rho(r)$ is in part because the potential reproduces the small surface energy difference
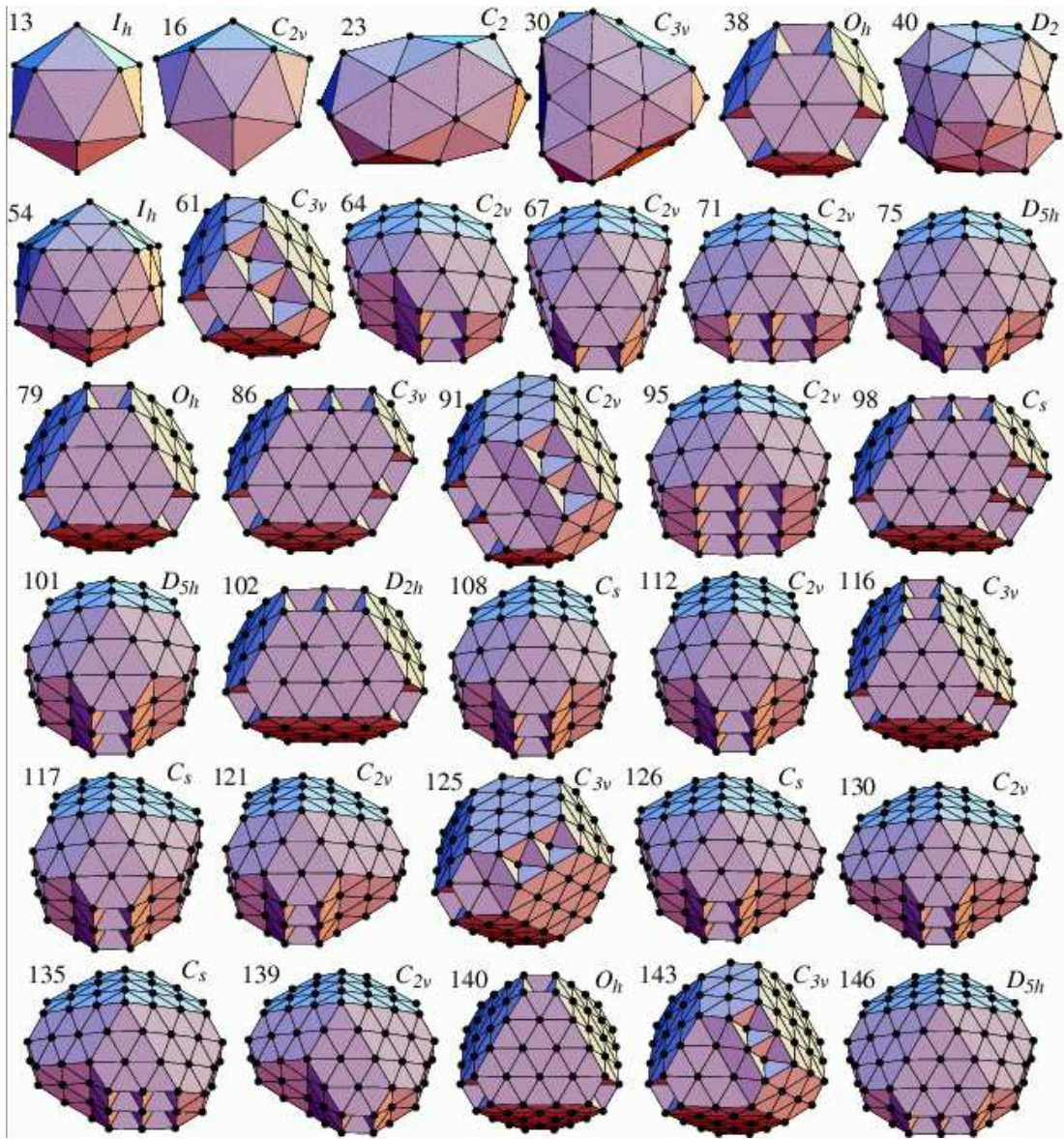
FIG. 3: A selection of clusters for lead clusters using the Gupta potential. Each structure is labelled by the size and point group.
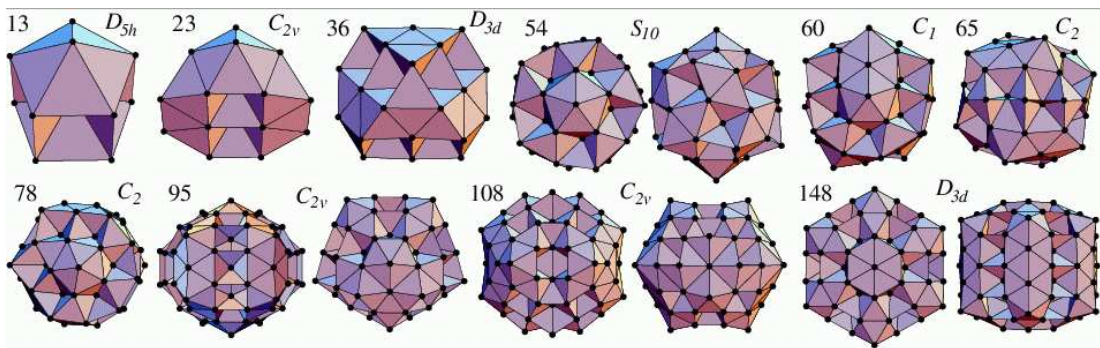

FIG. 4: A selection of particularly stable clusters for lead clusters using a glue potential.

TABLE I: Energies and point groups of the global minima for lead clusters modelled using a Gupta potential. For $N \geq 13$ a structural assignment has been made, where i stands for icosahedral, d for decahedral, fcc for face-centred cubic, cp for close-packed, dd for distorted decahedral and pt for polytetrahedral. If no assignment has been given the cluster has no apparent overall order.

N	PG	Energy		N	PG	Energy		N	PG	Energy		N	PG	Energy	
3	D_{3h}	-4.231623		40	D_2	-73.262766		77	C_{2v}	-144.258747	d	114	C_s	-215.807472	d
4	T_d	-6.099714		41	C_1	-75.112816		78	C_s	-146.128629	d	115	C_s	-217.749269	d
5	D_{3h}	-7.886887		42	C_s	-77.023173		79	O_h	-148.146432	fcc	116	C_{3v}	-219.694133	fcc
6	O_h	-9.755691		43	C_{2v}	-78.931871	d	80	C_{4v}	-150.013008	fcc	117	C_s	-221.691036	d
7	D_{5h}	-11.556399		44	C_2	-80.861958		81	C_{2v}	-151.930037	d	118	C_s	-223.559459	d
8	D_{2d}	-13.327553		45	C_1	-82.746570		82	C_{2v}	-153.841784	d	119	C_s	-225.523689	d
9	C_{2v}	-15.144569		46	C_3	-84.666164		83	C_{2v}	-155.720227	d	120	C_s	-227.470026	d
10	C_{3v}	-16.964625		47	C_1	-86.561578		84	C_s	-157.668905	d	121	C_{2v}	-229.493351	d
11	C_{2v}	-18.763846		48	C_1	-88.486884		85	C_s	-159.543391	d	122	C_{2v}	-231.398205	d
12	C_{5v}	-20.578513		49	C_1	-90.376393		86	C_{3v}	-161.564185	fcc	123	C_{2v}	-233.325446	d
13	I_h	-22.582269	i	50	D_{3h}	-92.296124	cp	87	C_s	-163.431365	fcc	124	C_{2v}	-235.254926	d
14	C_{6v}	-24.314590	pt	51	C_s	-94.162526	cp	88	C_s	-165.391034	fcc	125	C_{3v}	-237.188016	cp
15	D_{6d}	-26.251716	pt	52	C_{2v}	-96.110032		89	C_s	-167.258681	d	126	C_s	-239.203573	d
16	C_{2v}	-28.118745	dd	53	C_{3v}	-98.050794		90	C_s	-169.211406	fcc	127	C_s	-241.071732	d
17	C_{2v}	-29.970808	dd	54	I_h	-100.007540	i	91	C_{2v}	-171.177663	cp	128	C_s	-243.041253	d
18	C_s	-31.807535	dd	55	I_h	-101.835280	i	92	C_s	-173.043249	cp	129	C_s	-244.983046	d
19	C_s	-33.630069	dd	56	D_{2h}	-103.745751	fcc	93	C_1	-174.999552	cp	130	C_{2v}	-247.006258	d
20	C_s	-35.455114	dd	57	C_{2v}	-105.662759	d	94	C_s	-176.951443	cp	131	C_{2v}	-248.910730	d
21	C_{6v}	-37.331154	pt	58	C_1	-107.560437		95	C_{2v}	-178.892736	d	132	C_s	-250.839600	d
22	C_s	-39.259153		59	C_{2v}	-109.458501	d	96	C_s	-180.777213	cp	133	C_s	-252.753620	d
23	C_2	-41.158169		60	C_{2v}	-111.406643	d	97	C_s	-182.761992	d	134	C_1	-254.691944	d
24	C_s	-43.011299		61	C_{3v}	-113.381653	cp	98	C_s	-184.740639	fcc	135	C_s	-256.715113	d
25	C_1	-44.836233		62	C_s	-115.247146	cp	99	C_s	-186.654481	d	136	C_{4v}	-258.635983	fcc
26	C_s	-46.711166		63	C_s	-117.178015	cp	100	C_{5v}	-188.605832	d	137	C_s	-260.551431	d
27	C_s	-48.618276		64	C_{2v}	-119.187860	d	101	D_{5h}	-190.629737	d	138	C_s	-262.495627	d
28	C_1	-50.525086		65	C_{2v}	-121.058816	d	102	D_{2h}	-192.543687	fcc	139	C_{2v}	-264.518644	d
29	C_2	-52.420240		66	C_s	-122.990751	d	103	C_{2v}	-194.458602	d	140	O_h	-266.440716	fcc
30	C_{3v}	-54.337045		67	C_{2v}	-124.922594	d	104	C_{2v}	-196.367268	fcc	141	C_{2v}	-268.353333	d
31	C_3	-56.148062		68	C_{3v}	-126.812603	cp	105	C_{2v}	-198.306531	d	142	C_s	-270.260176	d
32	D_{2d}	-58.061383		69	C_1	-128.726858	d	106	C_s	-200.237783	d	143	C_{3v}	-272.223375	cp
33	C_1	-59.923961		70	C_s	-130.690514	d	107	C_s	-202.155252	cp	144	C_s	-274.213617	d
34	C_2	-61.841131		71	C_{2v}	-132.710251	d	108	C_s	-204.178302	d	145	C_{5v}	-276.170441	d
35	C_{2v}	-63.721030		72	C_s	-134.580108	d	109	C_s	-206.044130	d	146	D_{5h}	-278.193661	d
36	C_2	-65.627949		73	C_s	-136.507283	d	110	C_s	-208.009245	d	147	C_s	-280.051292	d
37	C_{2v}	-67.555415	dd	74	C_{5v}	-138.466765	d	111	C_s	-209.955620	d	148	C_{2v}	-282.029242	d
38	O_h	-69.488671	f	75	D_{5h}	-140.489863	d	112	C_{2v}	-211.979029	d	149	C_s	-283.886484	d
39	C_{4v}	-71.356501	f	76	C_{2v}	-142.358601	d	113	C_{2v}	-213.884008	d	150	C_{2v}	-285.864042	d

between the fcc {111} and {100} faces of lead.[4] Although an atom on a {100} faces has one less nearest neighbour, this is in part compensated because it has more next-neighbours at $\sqrt{2}r_0$ that make a significant contribution to $\rho(r)$. For the clusters this does not lead to {100} facets but most of the surfaces of the clusters involve some combination of squares and triangles.

That more disordered structures are favoured for the glue potential compared to the Gupta potential is sim-ply because of the greater dominance of the embedding term. However, the reasons why the glue global minima have the best embedding energy is more subtle. In particular, it is related to the position of the cutoff, which occurs between the second and third neighbour shells of the ordered structures. By comparison the disordered clusters have a much broader spectrum of pair distances, and it is in fact the contributions to the $\bar{\rho}_i$ values from distances near to the cutoff that tip the balance in favour

of the observed structures.[2] The position of this cutoff is not physically motivated, but has been chosen for computational convenience. As the structures do not seem to reflect robust features of the potential, they showed be viewed with appropriate skepticism.

Unfortunately, experiments on the structure of lead clusters are few. There have been some mass spectroscopic studies of very small clusters, but these are in the size range $(N < 25)$,[18,19] where empirical potentials are expected to be least applicable. The most relevant experiments are those by Hyslop *et al.* using electron diffraction.[20] However, for the size range most relevant to the present study, no adequate fit to the diffraction patterns was possible, whereas the larger clusters appear to be dominated by decahedra.

IV. CONCLUSIONS

It is the contention of this paper that to make progress in predicting the structure of clusters, understanding the relationship between the interactions and the resulting structure is important. Such an approach will provide a better general framework for understanding the criteria for a potential to be successful, and specific insights into the utility of a particular potential.

That the two lead potentials we consider suggest a to-tally different pattern of structures illustrates some of the problems for predicting cluster structure. However, given the differences in the potentials when compared in their effective pair format, the resulting structural differences are not in themselves so surprising.

The results also illustrate some of the pros and cons of using potentials with a specified form as with the Gupta potential, versus those with flexible forms. The former have less opportunity to produce manifestly unreasonable structures, but this is because of their more limited range of structural behaviour. If the real structures lie outside of this range, then such potentials have no chance of successful structural prediction. For example, the Gupta potential predicts that decahedral structures dominate at the larger sizes in this study, whereas the experimental electron diffraction suggest none of the standard forms.[20]

In contrast, flexible potentials have more chance of predicting some of the unusual structures that may occur at small sizes. However, there can be unforeseen consequences in regions of configuration space that lie outside of the possibilities considered in the fitting process. In the current case, the lead glue clusters are able to exploit questionable features of the potential, and so the structures are probably not realistic. This is not because this potential is a bad one—it has been widely used with reasonable success. Rather, it illustrates how predicting cluster structures is a very stringent test of a potential.

[*] Electronic address: jpkd1@cam.ac.uk

[1] J. P. K. Doye and F. Calvo, Phys. Rev. Lett. **86**, 3570 (2001).

[2] J. P. K. Doye and S. C. Hendy, Eur. Phys. J. D **22**, 99 (2003).

[3] F. Cleri and V. Rosato, Phys. Rev. B **48**, 22 (1993).

[4] H. S. Lim, C. K. Ong, and F. Ercolessi, Surf. Sci. **269/270**, 1109 (1992).

[5] R. A. Johnson and D. J. Oh, J. Mater. Res. **4**, 1195 (1989).

[6] J. P. K. Doye, D. J. Wales, and R. S. Berry, J. Chem. Phys. **103**, 4234 (1995).

[7] K. Michaelian, N. Rendón, and I. L. Garzón, Phys. Rev. B **60**, 2000 (1999).

[8] J. M. Soler, M. R. Beltrán, K. Michaelian, I. L. Garzón, P. Ordejón, D. Sánchez-Portal, and E. Artacho, Phys. Rev. B **61**, 5771 (2000).

[9] J. M. Soler, I. L. Garzón, and J. D. Joannopoulos, Solid State Commun. **117**, 621 (2001).

[10] F. Baletto, R. Ferrando, A. Fortunelli, F. Montalenti, and C. Mottet, J. Chem. Phys. **116**, 3856 (2002).

[11] J. P. K. Doye, J. Chem. Phys. **119**, 1136 (2003).

[12] J. P. K. Doye, Phys. Rev. B **68**, 195418 (2003).

[13] D. J. Wales and J. P. K. Doye, J. Phys. Chem. A **101**, 5111 (1997).

[14] D. J. Wales, J. P. K. Doye, A. Dullweber, M. P. Hodges, F. Y. Naumkin, F. Calvo, J. Hernández-Rojas and T. F. Middleton, The Cambridge Cluster Database, http://www-wales.ch.cam.ac.uk/CCD.html.

[15] S. K. Lai, P. J. Hsu, K. L. Wu, W. K. Liu, and M. Iwamatsu, J. Chem. Phys. **117**, 10715 (2002).

[16] L. L. Boyer and J. Q. Broughton, Phys. Rev. B **42**, 11461 (1990).

[17] J. P. K. Doye and D. J. Wales, New J. Chem. **22**, 733 (1998).

[18] J. Mühlbach, P. Pfau, K. Sattler, and E. Recknagel, Phys. Lett. A **87**, 415 (1982).

[19] K. LaiHing, R. G. Wheeler, W. L. Wilson, and M. A. Duncan, J. Chem. Phys. **87**, 3401 (1987).

[20] M. Hyslop, A. Wurl, S. A. Brown, B. D. Hall, and R. Monot, Eur. Phys. J. D **16**, 233 (2001).